

# Albedo on cropland: Field-scale effects of current agricultural practices in Northern Europe



Petra Sieber<sup>1,\*</sup>, Sepp Böhme, Niclas Ericsson, Per-Anders Hansson

*Department of Energy and Technology, Swedish University of Agricultural Sciences (SLU), Uppsala SE750 07, Sweden*

## ARTICLE INFO

### Keywords:

Land management  
Biophysical  
Radiative forcing  
Climate impact  
LCA  
Life cycle assessment

## ABSTRACT

Agricultural land use and management affect land surface albedo and thus the climate. Increasing the albedo of cropland could enhance reflection of solar radiation, counteracting the radiative forcing (RF) of greenhouse gases (GHGs) and local warming. However, knowledge is lacking on how agricultural practices affect albedo under local conditions, and on the benefits of individual practices. In this study, field measurements were made in 15 paired plots at a site in Northern Europe to determine albedo, net shortwave irradiance and RF impacts under various common crops, cultivation intensities and tillage practices. Field data for 2019–2020 were compared with satellite-based albedo for the surrounding region in 2010–2020. At regional level, different combinations of soil type, yearly weather and agricultural practices led to great variability in the albedo of individual crops, despite similar pedo-climatic conditions. At field level within years, albedo differences were determined mainly by crop type, species-specific phenology and post-harvest management. Annual albedo was higher with perennial ley (0.20–0.22) and winter-sown crops (0.18–0.22) than with spring-sown crops (0.16–0.18) and bare soil (0.13). Barley had the highest albedo among winter and spring cereals. In summer, when increased albedo could alleviate local heat stress, oats reduced net shortwave irradiance at the surface by 0.8–5.8 W m<sup>-2</sup> compared with other cereals, ley, peas or rapeseed. Delayed or reduced tillage gave high local cooling potential (up to -13.6 W m<sup>-2</sup>) in late summer. Potential benefits for global mean climate as GWP<sub>100</sub> per hectare and year reached -980 kg CO<sub>2</sub>e for avoiding black fallow, -578 kg CO<sub>2</sub>e for growing a winter-sown variety and -288 kg CO<sub>2</sub>e for delayed tillage. Thus realistic albedo increases on cropland could have important effects on local temperatures and offset a substantial proportion of the RF deriving from field-scale GHG emissions on short time-scales.

## 1. Introduction

Land surface albedo, i.e. the fraction of solar radiation reflected back from the ground, is important for climate regulation at local to global scale (Anderson-Teixeira et al., 2012; Mahmood et al., 2014; Pielke et al., 1998). Increased albedo leads to a reduction in net shortwave irradiance at the surface and at the top of the atmosphere (TOA), with the potential to cool local, regional and global mean temperatures (Bala et al., 2007; Betts et al., 2007; Davin & de Noblet-Ducoudré, 2010). Albedo management on agricultural land has been proposed as a way to counteract the radiative forcing (RF) and climate impacts of elevated greenhouse gas (GHG) concentrations. Increasing the reflectivity of cropland and grassland could help rectify the Earth's current and potential future radiative imbalance, although the global-scale potential is

modest due to the limited areal and seasonal extent of such modifications (Lenton & Vaughan, 2009; Singarayer & Davies-Barnard, 2012). At field scale, albedo change can substantially improve or impair the net negative RF achieved by carbon sequestration practices and crop-based biofuels (Kaye & Quemada, 2017; Smith, 2016; Smith et al., 2016). This has spurred the development and application of life cycle assessment (LCA) methods that include both GHGs and albedo, since LCA is widely used in policies to evaluate the climate performance of biofuels (Bright et al., 2012; Cai et al., 2016; Caiazzo et al., 2014; Sieber et al., 2020).

Cropland albedo management can be a viable and effective option for regional adaptation to climate change (Seneviratne et al., 2018; Singarayer & Davies-Barnard, 2012). Agricultural land and densely populated areas are especially vulnerable to extreme temperatures and drought. Increasing surface albedo by 0.1 could reduce regional

\* Corresponding author at: Department of Energy and Technology, Swedish University of Agricultural Sciences (SLU), PO Box 7032, Uppsala SE750 07, Sweden  
 E-mail addresses: [petra.sieber@env.ethz.ch](mailto:petra.sieber@env.ethz.ch) (P. Sieber), [sepp.bohme@slu.se](mailto:sepp.bohme@slu.se) (S. Böhme), [niclas.ericsson@slu.se](mailto:niclas.ericsson@slu.se) (N. Ericsson), [per-anders.hansson@slu.se](mailto:per-anders.hansson@slu.se) (P.-A. Hansson).

<sup>1</sup> Present address: Institute for Atmospheric and Climate Science, ETH Zurich, Zurich, Switzerland.

warming by up to 1°C in terms of mean annual temperature and up to 2–3°C in terms of annual maximum daytime temperature (Seneviratne et al., 2018). The cooling effect is amplified during extreme heat events, because albedo increase is most effective on clear summer days with high incoming radiation, and it preserves soil moisture throughout the year, leading to evaporative cooling under hot, dry conditions (Davin et al., 2014; Wilhelm et al., 2015). Thus albedo management could alleviate heat stress and summer drought in agricultural regions (Doughty et al., 2011; Wilhelm et al., 2015). Cooler soil microclimates during summer can also reduce organic matter decomposition and potentially enhance soil carbon stocks (von Haden et al., 2019).

The albedo of natural surfaces depends on the physiology and structure of plant cover, soil texture and organic matter content, and local meteorology (Bonan, 2015; Bright et al., 2015; Sieber et al., 2019). Albedo is well-characterised by land cover type, such as the 17 classes in the International Geosphere-Biosphere Programme (IGBP), using satellite observations to capture spatial and seasonal variation (Gao et al., 2014). However, data gaps and uncertainty remain about how land use and management within classes such as cropland and grassland influence albedo, depending on soil properties and local climate (Erb et al., 2017). The albedo of cropland is particularly variable due to various agricultural practices and annual cultivation cycles with rapid changes in vegetation and the fraction of exposed soil (Cescatti et al., 2012; Gao et al., 2005). Growing vegetation cover can increase or decrease albedo, depending on the albedo of bare soil (~0.05–0.40) in relation to that of the vegetation and the effect of vegetation on soil moisture (Bonan, 2015). Plant characteristics lead to differences in albedo between crop species and varieties, depending on canopy morphology, foliage nitrogen and chlorophyll concentration, leaf trichomes, glaucousness and waxiness (Genesio et al., 2021; Hollinger et al., 2010; Singarayer & Davies-Barnard, 2012). Albedo is also affected by management practices such as tillage, residue retention and fallowing (Davin et al., 2014; Liu et al., 2021), application of organic amendments (e.g. manure, digestate, biochar), cover cropping or intercropping (e.g. Carrer et al., 2018; Miller et al., 2016; Seneviratne et al., 2018 and references therein). Choice, combination and timing of management practices can lead to substantial variations in albedo between individual fields and measuring occasions. In the literature, albedo of various crops is reported for full vegetation cover (Monteith & Unsworth, 2013) or as minimum and maximum values (Breuer et al., 2003). However, information on the seasonal patterns of albedo is needed to estimate accumulation of net shortwave irradiance on seasonal or annual time scales and to assess the overall climate impact of crops or management practices.

Satellite-based data comprise long-term records of albedo at global scale and are useful for monitoring spatial and temporal variations in albedo (Qu et al., 2015). The Moderate Resolution Imaging Spectroradiometer (MODIS) albedo product is frequently used to characterise the albedo of contrasting land cover types, due to its daily resolution (Gao et al., 2014; Wang et al., 2018). However, it is challenging to match the gridded composite product (which is the output of a spatial and temporal sampling procedure) with surface conditions, particularly in heterogeneous agricultural landscapes (Duveiller et al., 2011; Sieber et al., 2022). Crop fields are often smaller than the observational footprint of satellite pixels, resulting in a mixed signal that does not characterise a single crop or management regime. Field-based measurements are needed for local, crop-specific and management-specific characterisation of surface albedo. The global FLUXNET network includes over 500 micrometeorological stations located on cropland, representing different pedo-climatic conditions and often multiple years. However, few albedo measurements are available for paired sites with similar environmental conditions, but different cropland management. It is therefore difficult to identify the effects of agricultural management on albedo and distinguish them from the influence of soil properties, local climate and yearly weather. To overcome this knowledge gap, in this study we carried out field measurements of albedo in an experiment designed specifically to analyse differences between agricultural land

uses and management practices.

The aim of the study was to investigate the effects of current agricultural land use and management practices in specific fields on the albedo of cropland, and thereby the climate. Field measurements of incoming and reflected radiation were used to analyse how albedo differed between crop species, cultivation intensities and tillage practices on seasonal time scales. A mobile system was developed for measuring albedo on 14 plots on the same day throughout one year. The potential impacts of albedo change on climate were quantified as change in net shortwave irradiance at the surface and TOA, global annual mean RF and global warming potential (GWP). Such data help understand the potential magnitude of effect and can be included in LCAs of crop production for food or bioenergy.

## 2. Materials and methods

### 2.1. Field sites

Field albedo measurements were conducted in 2019–2020 at four sites (Ultuna, Ulleråker, Kungsängen, Lövsta) lying close to each other in Uppsala (59.82°N, 17.65°E), central Sweden (Fig. 1). Of these, Ultuna is an experimental site and the other sites are commercially farmed. The climate in Uppsala is humid-temperate, with cold winters and mild to warm summers. During the measurement period (26 Sep 2019–30 Sep 2020), mean temperature in the region was 8.4°C, mean precipitation was 519 mm and mean global radiation was 119 Wm<sup>-2</sup> (Table 1). The weather in the study period was warmer and drier than average, and Uppsala had particularly few days with snow cover (16, compared with 80 days on average). Arable soils in Uppsala (Swedish National Soil and Crop Inventory 2001–2007, n=35) were classified mostly as clay, clay loam, silty clay and silty clay loam with mean (standard deviation, SD) contents of 42% (12%) clay, 40% (11%) silt, 18% (18%) sand and 4.6% (2.0%) organic matter in the topsoil (0–20 cm). Soil samples taken at the Ultuna experimental site (analysis 2018–2019, n=41) included silty clay and silty clay loam, with 45% (6%) clay, 18% (5%) sand and 1.7% (0.7%) organic matter content.

Albedo was measured on 15 plots with crop species and management regimes commonly found in Northern Europe (Table 2). The study included four winter-sown crops (wheat, rye, barley, rapeseed), four spring-sown crops (wheat, barley, oats, peas), three types of grass-clover ley (clover-dominated, grass-dominated, extensive), bare soil and two replicates. Field operations and inputs per crop followed normal practice in conventional cropping. Plots with annual crops (except spring barley and peas, which were covered by residues of the preceding rapeseed and wheat crop, respectively) were ploughed in early September 2019 before the measurements started. Shallow tillage was performed in late September 2019 and all plots were harrowed shortly before sowing. After harvest in August 2020, the timing of tillage operations varied depending on the subsequent crop (Table 2). Nutrients were applied as mineral fertiliser and, additionally, biogas digestate was applied to ley grass (17 April 2020) and winter rapeseed (25 June 2020).

The bare soil plot was kept free from weeds by regular machine passes during the growing season (Table 2). The southern (S) Ultuna field was first split into separate plots for bare soil, spring wheat and oats after the cereals had been sown in April 2020. Until then, one measurement was taken to represent unvegetated plots at Ultuna S. The three types of grass-clover ley differed in terms of age and management regime (e.g. fertilisation and number of cuts per year), leading to different species composition and surface properties in the study period. Ley clover had been undersown in the preceding cereal crop, was not fertilised and cut twice in the study period. Ley grass had been established three years earlier, was fertilised intensively and cut 3–4 times per year. Two management alternatives were considered for ley grass in the study period, continued cultivation with three cuts or termination in early August 2020 after two cuts. Ley extensive was measured on 6-year old ley that was not fertilised in the study year and cut only twice by



**Fig. 1.** Location of the four measurement sites in Uppsala, Sweden. Ultuna had a northern and southern field, Ulleråker had a western and eastern field, and Kungsängen and Lövsta had one field each. Image Landsat/Copernicus, map data © 2021 Google.

**Table 1**

Mean monthly and annual meteorological values for Uppsala during the measurement period (2019–2020) and 30-year (mean) values obtained from the nearest weather station in Uppsala ([celsius.met.uu.se](http://celsius.met.uu.se)).

	Air temperature [°C]	Precipitation [mm]	Global radiation [Wm <sup>-2</sup> ]	Snow cover [days]	Max snow depth [cm]	
2019- 2020	Mean	2019- 2020	Mean	2019-2020	2019- 2020	2019- 2020
Oct	6.2	6.5	61.7	53.1	42.9	0
Nov	2.6	1.8	67.5	52.9	13.2	5
Dec	1.7	-1.7	67.9	45.5	6.1	7
Jan	3.5	-2.7	15.2	39.3	12.6	0
Feb	2	-2.8	22.6	29.7	39.2	2
Mar	2.8	0.2	26.4	32.6	95.2	1
Apr	6.5	5.2	16.7	31.7	174.9	3
May	9.2	10.9	41.3	38.7	224.5	0
Jun	18.4	14.7	54.9	61	290.2	0
Jul	16.1	17.7	89.2	65.1	226.9	0
Aug	18.2	16.2	19.9	73.6	202.3	0
Sep	13.1	11.4	35.8	52.4	102.8	0
Year	8.4	6.5	519.1	575.6	119.2	16
						13

mowing and topping, respectively. The vegetation was an inhomogeneous mix of clover, grasses and weeds, used for biogas production.

## 2.2. Field measurements

Incoming and reflected shortwave irradiance was measured with a pair of pyranometers (CMP6, Kipp & Zonen, Delft, the Netherlands), which measure radiation in the 285–2800 nm spectral range over a 180° field of view. The downward-facing sensor was equipped with a glare screen to limit its field of view to 170° and thus prevent direct illumination at low sun angles. The pyranometers were mounted back-to-back and installed on a portable tripod with a vertically extendable mast and a 2 m long horizontal crossarm (Fig. 2). The sensors were positioned 1.5 m above the vegetation canopy in each plot, so that a circular area with 15 m radius generated 99% of the downward-facing sensor's signal. The height was adjusted for each crop and measurement, using the extendable mast and legs of the tripod. The sensors were levelled by means of two perpendicular spirit levels gauging pitch and roll. The pyranometers were connected to a data logger (CR300, Campbell Scientific), which recorded their signals separately as 10-second average irradiance in Wm<sup>-2</sup>. A Bluetooth serial adapter was installed to transmit the data directly in the field and monitor the measurements.

Measurements were made every 1–2 weeks under stable (ideally clear-sky) conditions within three hours of solar noon. Each plot was sampled for 3–5 minutes, or longer if the signal was temporarily unstable due to clouds or changing cloudiness. The sampling design was based on previous evaluations of continuous pyranometer data, which indicate

that measuring for a few minutes under direct sunlight provides representative shortwave fluxes to approximate daily albedo (Williamson et al., 2016) and that selectively measured albedo on clear days around solar noon can be used to approximate seasonal albedo for energy balance calculations (Sieber et al., 2019). The measurement frequency was increased in April–September (usually every 7–9 days) to capture changes in vegetation and soil properties under elevated incoming solar radiation. Fewer measurements were taken during the rest of the year (usually every 12–14 days), due to frequently cloudy conditions and less significant albedo changes under low levels of incoming solar radiation.

Albedo for each plot and sampling day was calculated as the ratio of reflected to incoming average irradiance under stable conditions. A stable period (at least 30 seconds, usually 2–4 minutes) was identified based on incoming irradiance measured by the upward-facing pyranometer and continuous observations from a meteorological station on the northern Ultuna field. Individual missing measurements were replaced by albedo values deriving from close observations in time or similar plots. Field-measured albedo was interpolated to daily frequency using the Akima method, a polynomial spline with locally determined slopes that avoids overshooting (Akima, 1970).

## 2.3. Shortwave irradiance and climate impact

Albedo controls the shortwave flux leaving the Earth's surface ( $SW_{Surf\downarrow}$ ), a component of the surface energy balance. This flux partially escapes through the atmosphere. Surface albedo thereby acts on up-welling shortwave irradiance at the TOA ( $SW_{TOA\uparrow}$ ), which is an important component of the global energy balance. The higher the incoming solar irradiance at the surface ( $SW_{Surf\downarrow}$ ) and the atmospheric transmittance, the greater the contribution of surface albedo to  $SW_{TOA\uparrow}$ . Incoming irradiance and atmospheric transmittance vary with solar angle and cloudiness, and are typically high on clear summer days. Incoming irradiance is enhanced over surfaces with high albedo, due to multiple reflections between surface and atmosphere. A single-layer atmosphere model was used to estimate  $SW_{Surf\downarrow}$  and  $SW_{TOA\uparrow,Surf}$  as a function of surface albedo (Stephens et al., 2015; Winton, 2005):

$$SW_{Surf\downarrow}(\alpha) = SW_{TOA\uparrow} \frac{\tau}{1 - \alpha r} \quad (1)$$

$$SW_{TOA\uparrow,Surf}(\alpha) = \underbrace{SW_{Surf\downarrow}(\alpha) * \alpha * \tau}_{SW_{Surf\downarrow}(\alpha)} \quad (2)$$

where  $\tau$  is single-pass atmospheric transmittance of incoming and reflected radiation and the denominator ( $1 - \alpha r$ ) represents multiple reflections between a surface with albedo  $\alpha$  and the atmosphere with reflectivity  $r$ . Atmospheric properties were assumed constant on all passes of radiation through the atmosphere (i.e. independent of downward/upward direction and previous interactions). With this simplification, transmittance and reflectivity can be calculated from four boundary fluxes Eqs. 3 and (4) (Winton, 2005). Data on the boundary

**Table 2** Crop, variety and management regime in plots at the four field sites. Nitrogen fertiliser rate in kg N ha<sup>-1</sup>. N/S/E/W = northern/southern/eastern/western field, D = biogas digestate application, P = ploughing (deep tillage), C = cultivation (shallow/reduced tillage), T = terminated, TP = topped.

Plot	Variety	Site and field	N rate	Tillage before		Sowing	Harvesting	Tillage after
Winter wheat	Norin	Ultuna N	180	5 Sep 2019 (P), 12 Sep 2019 (C)	13 Sep 2019	7 Aug 2020 (C)	8 Aug 2020 (C)	
Rye	Bintto	Ultuna N	130	5 Sep 2019 (P), 12 Sep 2019 (C)	13 Sep 2019	7 Aug 2020 (P)	28 Sep 2020 (P)	
Winter barley	Joker	Ultuna S	120	5 Sep 2019 (P), 6 Sep 2019 (C)	6 Sep 2019	6 Aug 2020 (C)	8 Aug 2020 (C)	
Winter rapsseed	SV Florian	Lövsta	170 (D)	6 Aug 2019 (C)	7 Aug 2019	16 Aug 2020 (C)	6 Sep 2020 (C)	11 Sep 2020 (C)
Spring wheat	Quarina	Ultuna S	120	5 Sep 2019 (P), 6 Nov 2019 (C), 6 Apr 2020 (C)	11 Apr 2020	23 Aug 2020 (C)	31 Aug 2020 (C)	21 Sep 2020 (C)
Spring barley	Planet	Ultuna N	120	27 Sep 2019 (C), 6 Apr 2020 (C)	11 Apr 2020	23 Aug 2020 (P)	28 Sep 2020 (P)	
Oats	Guld	Ultuna S	100	5 Sep 2019 (P), 6 Nov 2019 (C), 6 Apr 2020 (C)	11 Apr 2020	23 Aug 2020 (C)	31 Aug 2020 (C)	21 Sep 2020 (C)
Peas	Ingrid	Ultuna N	0	27 Sep 2019 (C), 6 Apr 2020 (C)	9 Apr 2020	23 Aug 2020 (C)	31 Aug 2020 (C)	7 Sep 2020 (C)
Ley clover	Mira 21 grass-clover	Ultuna N	0	–	2019	8 Jun 2020, 1 Aug 2020,	–	–
Ley grass	Mira 21 grass-clover	Kungsängen	125 (D)	–	2016	2 Jun 2020, 10 Jul 2020,	–	–
Ley grass T	Mira 21 grass-clover	Kungsängen	125 (D)	–	2016	5 Aug 2020, 2 Jun 2020,	–	6 Aug 2020 (P)
Ley extensive	Unknown grass-clover	Ulleråker W	0	–	2014	10 Jul 2020, 16 Jun 2020,	–	–
Bare soil	–	Ultuna S	0	5 Sep 2019 (P), 6 Sep 2019 (C), 6 Apr 2020 (C)	–	5 Aug 2020 (TP)	–	–
Rye	Bintto	Ultuna S	120	5 Sep 2019 (P), 6 Sep 2019 (C)	6 Sep 2019	6 Aug 2020 (C)	8 Aug 2020 (C)	31 Aug 2020 (C)
Ley extensive	Unknown grass-clover	Ulleråker E	0	–	2014	16 Jun 2020, 4 Aug 2020 (TP)	–	–

fluxes, i.e. downwelling and upwelling shortwave radiation at the surface and TOA, were obtained from the ERA5 global reanalysis dataset (Hersbach et al., 2018) at the nearest grid point to the field sites.

$$\tau = \frac{SW_{TOA\downarrow} SW_{Surf\downarrow} - SW_{TOA\uparrow} SW_{Surf\uparrow}}{SW_{TOA\downarrow}^2 - SW_{Surf\downarrow}^2} \quad (3)$$

$$r = \frac{SW_{TOA\downarrow} SW_{TOA\uparrow} - SW_{Surf\downarrow} SW_{Surf\uparrow}}{SW_{TOA\downarrow}^2 - SW_{Surf\downarrow}^2} \quad (4)$$

The direct effect of albedo on net shortwave irradiance (i.e. not including effects of rapid adjustments in the troposphere, such as cloud formation) at the surface is given by Equation 5. The direct effect at the TOA, which consists of contributions of atmospheric reflectivity and surface albedo, is given by Equation 6.  $SW_{TOA\downarrow, Surf}$  was calculated daily to capture the seasonal covariation of albedo, irradiance and atmospheric transmittance (Sieber et al., 2019), and then aggregated to annual resolution. The impact of albedo change on Earth's global energy budget was expressed as global annual average instantaneous RF ( $RF = A/A_E * \Delta SW_{TOA,\text{net}}[y]$ ), where  $A$  is the area affected by albedo change (here  $A = 1 \text{ ha} = 10^4 \text{ m}^2$ ) in relation to the Earth's surface area ( $A_E = 5.1 \times 10^{14} \text{ m}^2$ ). Radiative forcing is the basis for commonly used metrics to quantify the impact of albedo change on global mean climate, including temperature change, GWP and other CO<sub>2</sub>-equivalence metrics (Bright & Lund, 2021; Bright et al., 2015; Sieber et al., 2020). Here, GWP was calculated with alternative time horizons of 100 or 20 years, using the methods described in Sieber et al. (2020). Per unit (1 Wm<sup>-2</sup>) and year of RF from albedo change, GWP<sub>100</sub> was  $10.9 \times 10^{12} \text{ kg CO}_2\text{e}$  and GWP<sub>20</sub> was  $40.1 \times 10^{12} \text{ kg CO}_2\text{e}$ .

$$SW_{Surf,\text{net}}(\alpha) = (1 - \alpha)SW_{Surf\downarrow}(\alpha) \quad (5)$$

$$SW_{TOA,\text{net}}(\alpha) = (1 - r) SW_{TOA\downarrow} - SW_{TOA\uparrow, Surf}(\alpha) \quad (6)$$

Annual albedo is defined as the ratio of reflected to incoming average irradiance over the year, i.e.  $\alpha[y] = SW_{Surf\downarrow}(\alpha)[y]/SW_{Surf\uparrow}(\alpha)[y]$ . Using the discontinuous measurements available here, it can be calculated as the average of daily albedo weighted by daily mean surface irradiance:  $\alpha[y] = \sum \alpha[d]*SW_{Surf\downarrow}(\alpha)[d] / \sum SW_{Surf\downarrow}(\alpha)[d]$ .

## 2.4. Uncertainty analysis

### 2.4.1. Measurement uncertainty

Sources of uncertainty in field-level albedo included instrument errors, imprecise positioning and levelling of sensors in the field and inhomogeneity within sampled plots. The combined uncertainty was estimated from 45 repeated measurements, taken at five equally spaced points (12 m distance) within each of nine different plots on 31 May 2020. These plots differed in terms of crops grown, growth stages and management regime. The variance of the random error was assumed independent of crop and day of year. Error sources may however vary in reality, due to e.g. greater instrument errors under low incoming irradiance and extreme temperatures, increasing difficulty in positioning and levelling the sensors in high, dense vegetation and varying inhomogeneity at different growth stages. Measurement uncertainty was estimated as SD calculated from albedo values in the 45 sampling points with plot means subtracted. The calculated uncertainty was applied to measured albedo values and propagated into output variables (interpolated daily albedo, annual albedo,  $SW_{Surf,\text{net}}$ ,  $SW_{TOA,\text{net}}$ , RF, GWP) using Monte Carlo simulation with Latin hypercube sampling and 10,000 runs.

### 2.4.2. Variations between adjacent fields

Two plots were included as replicates to assess the robustness of the data and possible differences in crop-specific albedo between adjacent fields. Replicates had the same crop varieties and similar growing conditions as the respective main plot, but were located in different fields (Table 2).



**Fig. 2.** Measurement set-up in cereal plots (left) during the growing season and (right) after harvest. The height of the pyranometer pair was adjusted using the extendable mast and legs of the tripod.

#### 2.4.3. Regional and inter-annual variations

The MODIS albedo product MCD43A1 v6 (Schaaf & Wang, 2015) was used for comparison with field-measured albedo and to assess variability across years and sites within a region. Albedo was obtained for crops harvested in 2011–2020 in Swedish agricultural production region PO4 (encompassing Uppsala county), which has characteristic production conditions in terms of topography, climate and soil type. Region PO4 has a humid-temperate climate, with mean annual temperature of 6.6°C, mean annual precipitation of 601 mm and clay and silty clay as prevalent soil types (Andrén et al., 2008). Methods to identify representative pixels per crop and to compute annual albedo were taken from Sieber et al. (2022). Accordingly, the ERA5 radiation data used for calculations with MODIS albedo were averaged regionally over region PO4 and temporally over the 10-year data period.

## 3. Results

### 3.1. Field-measured albedo values

Field-measured albedo ranged from 0.05 for non-vegetated plots in autumn to 0.95 for snow-covered plots in winter. During the growing season (Apr-Oct), albedo was 0.17–0.28 for perennial leys, 0.05–0.32 for winter cereals, 0.05–0.26 for spring cereals, 0.07–0.25 for peas and winter rapeseed, and 0.05–0.17 for the bare clay soil. The albedo of leys was high in autumn and spring and decreased over summer (Fig. 3). With annual crops, albedo increased as the plants developed because they were more reflective than the bare clay soil. The highest values were recorded shortly after harvest, for the reflective stubble and stalks of winter cereals (up to 0.32 on rye). The values were lower on plots where cultivation was performed directly after harvest, e.g. after light stubble cultivation it was 0.31 for rye (Ultuna S) and 0.27 for winter barley, while after two cultivations it was 0.19 for winter wheat (Fig. 4). Growing-season albedo was highest for rapeseed in the flowering stage (mid-May to early June) and for peas when the plants had matured and wilted in late June and July. Bare soil albedo varied depending on surface soil moisture content, which was affected by precipitation and temperature, and tillage. Albedo was 0.05–0.11 when the soil was moist and 0.13–0.16 when it was harrowed and dry in April–August. Measured and replaced albedo values are provided in Table S1 in Supplementary Material (SM).

In the repeated measurements, variability in individual plots was 1–4%, measured by the coefficient of variation (CV). Albedo values in the 45 sampling points are provided in Fig. S2 in SM. The estimated measurement uncertainty was SD 0.0045. Albedo values obtained on replicate plots (Fig. S3 in SM) were not suitable to assess measurement uncertainty, due to differences in species composition (extensive ley) or sowing and post-harvest management (rye) compared with the main

plots. The resulting variability was higher (SD 0.008 for extensive ley, SD 0.015 for rye) and differences consistent over time.

### 3.2. Seasonal patterns in albedo and net shortwave irradiance

Seasonal patterns in albedo and net shortwave irradiance can be expected to be similar for crops belonging to groups such as winter and spring crops, cereals and broadleaf crops or perennial leys. Comparisons between plots showed that this was generally true, although certain crop species and management practices led to distinct patterns in albedo (Fig. 5A–E) and  $SW_{Surf,net}$  (downwelling minus upwelling), primarily through changes in upwelling irradiance (Fig. 5F–J).

Substantial differences were observed between winter cereals, which affected large parts of the year (Fig. 5A,F). Winter barley (sown one week earlier) and rye developed faster than wheat and covered the dark soil better during autumn and spring. Among both winter and spring cereals, barley had the highest albedo during most of the growing season. Differences between spring crops were generally smaller during their short growing season (Fig. 5B,G). Before the establishment of spring crops, in September–April, albedo was higher for spring barley and pea plots than for spring wheat and oat plots due to shallow tillage and retained debris from the preceding crop. After harvest in August, high albedo on rye and winter barley plots with no or reduced tillage had strong impacts on  $SW_{Surf,net}$ . This effect was not seen for winter wheat, where two cultivations were performed directly after harvest to prepare the soil for the next crop. For spring cereals harvested later in August the effect of harvest on albedo was lower (0.24 for spring wheat and barley, 0.21 for oats), delayed and shorter. This led to a smaller impact on  $SW_{Surf,net}$ .

Winter wheat had higher albedo than spring wheat during autumn and spring, due to better soil coverage (Fig. 5C). The difference lasted until late June, when spring wheat had established a dense canopy and the albedo of winter wheat did not increase further. Impacts on  $SW_{Surf,net}$  were greatest in April–May (Fig. 5H). Winter rapeseed as a broadleaf crop and perennial ley provided even better coverage in autumn and spring, but the harvested plots were less reflective (Fig. 5D). This resulted in lower albedo in late summer, when the impact on  $SW_{Surf,net}$  is potentially high (Fig. 5I). Differences between leys due to age and management regime varied seasonally (Fig. 5E). The highest snow-free albedo value, 0.28, was recorded for ley clover in autumn. However, albedo was comparatively low throughout spring because clover is sensitive to cold temperatures. Intensively managed ley grass mostly had higher albedo than extensive ley in the main plot, but not in the replicate plot. Further seasonal differences were caused by harvesting, digestate application in April and termination of ley grass T by ploughing in August.

The effect of soil moisture on albedo was strongest for bare soil and

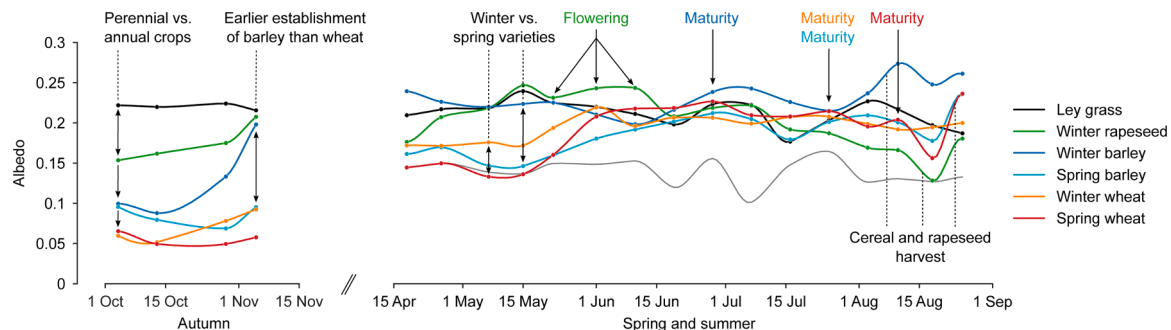


**Fig. 3.** Albedo on individual plots during the growing season in autumn and spring-summer. Coloured lines represent selected crops and the dark grey line is bare soil. Arrows for maturity mark the beginning of the maturity phase, when leaves and seeds start to turn yellow. Data include field-measured values (markers) and interpolated values (lines).

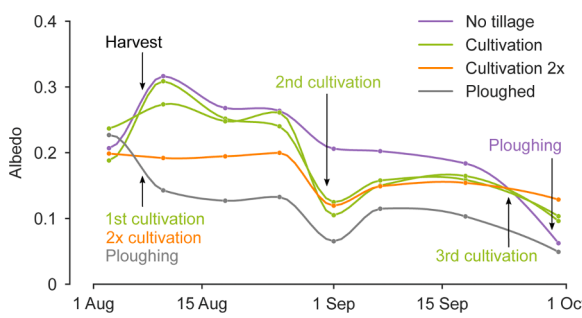


**Fig. 4.** Albedo on individual plots after harvest of winter cereals under different tillage intensity and timing. ‘No tillage’ was measured in the main rye plot, ‘Cultivation’ in rye (Ultuna S) and winter barley plots, and ‘Cultivation 2x’ in the winter wheat plot. Data for ‘Ploughed’ were taken from the ley grass T plot. Data include field-measured values (markers) and interpolated values (lines).

weaker for vegetated plots. Albedo with snow cover differed up to 0.29 between plots. However, snowfall in 2019–2020 was exceptionally low in Uppsala and occurred only during a period with low incoming radiation and low atmospheric transmittance (Dec–Feb), so that the effect on  $SW_{Surf,net}$  was small (Fig. 5F–J). The greatest differences in  $SW_{Surf,net}$  occurred on clear days around the summer solstice (20 Jun), between late May and mid-August for different plots relative to bare soil. During this time of the year, even small differences in albedo translated into strong forcings.

Main plots and replicates for rye showed similar albedo on fully-grown crops in June–August, but albedo of rye at Ultuna S was higher in April–May due to better establishment and lower in September due to earlier tillage (Fig. S3B in SM). These results indicate strong influence of management on field-level albedo. Main plots and replicates for extensive ley showed similar seasonal patterns (Fig. S3A in SM), but differences in albedo were typically around 0.01. Due to the age of the fields, varying shares of grass, weeds and clover had established, leading to great inhomogeneity within plots and differences between them. The main plot hosted coarser grasses and less clover than the replicate. Thus species composition can lead to substantial differences in field-level albedo for grass-clover ley.

### 3.3. Annual albedo and mean climate impacts

Annual albedo based on the field measurements was highest for winter barley (0.22), followed by ley (0.20–0.22), rye (0.21), winter rapeseed (0.20) and winter wheat (0.18) (Table 3). The lowest values among different types of ley and winter cereals were found on plots that were ploughed early, i.e. ley grass T and winter wheat. Spring cereals (0.17–0.18) and peas (0.16) had lower annual albedo than winter crops,

but clearly higher albedo than bare soil (0.13). Some of the albedo differences between plots were small and besides the crop grown, other sources of variability (e.g. management and species composition of ley, sowing and post-harvest management of rye) could have a large impact.

Uncertainties estimated by Monte Carlo simulation resulted in CV 0.4–0.7% for annual albedo, which is only a fraction of the uncertainty in individual measurements. The estimated effect of measurement uncertainty on climate impacts expressed as RF,  $GWP_{100}$  or  $GWP_{20}$  was CV 2–5%. The ranking of plots in terms of albedo and climate impacts (Table 3) was stable in ≥90% of the simulations for all pairs except ley clover-rye (Ultuna S), ley extensive-rye, ley grass T-winter rapeseed and spring wheat-oats (Table S4b in SM). For these pairs annual albedo differed by less than 0.001, with an uncertainty of SD 0.0009.

Annual albedo is not linearly related to mean climate impacts, due to covariance of albedo, solar irradiance and atmospheric transmittance on seasonal time scales. Thus the average climate impact per 0.01 albedo change was scenario-specific (i.e. dependent on the seasonal albedo patterns of the compared plots). In terms of  $GWP_{100}$ , for instance, it varied between 86 and 270 kg  $CO_2e\ ha^{-1}\ yr^{-1}$  for the studied land use and management options in Uppsala, excluding the four plot pairs with very small differences in albedo.

Annual albedo was almost 0.1 higher for winter barley than for bare soil. This resulted in lower calculated net shortwave irradiance at the surface ( $-8.0\ Wm^{-2}$ ) and at the TOA ( $-5.6\ Wm^{-2}$ ), excluding potential atmospheric feedbacks. Cultivation of winter barley on one hectare during one year, instead of keeping soil bare, could counteract RF of  $11 \times 10^{-11}\ Wm^{-2}$  (averaged globally), which is equivalent to the cumulative RF exerted by an emission pulse of 1202 kg  $CO_2$  over 100 years (using  $GWP_{100}$ ) or 4418 kg  $CO_2$  over 20 years (using  $GWP_{20}$ ). The shorter the time horizon of interest, the higher the relative importance of the short-term radiative perturbation caused by albedo change. Within the same year, the albedo effect was equivalent to RF of 65 Mg  $CO_2$ . However, comparing the impact of climate forcers over a one-year time horizon is not common and ignores the RF of GHGs in later years, due to their long perturbation lifetime.

Relative to bare soil, even the crop with the lowest albedo, peas, had a global climate benefit of -411 kg  $CO_2e$  using  $GWP_{100}$ . Bare soil was useful as a reference in this study because it represented the possible lower limit for albedo on most measurement days and in the annual mean. Moreover, the data can be used to estimate the potential benefit of avoiding temporary black fallow on unused cropland (-980 kg  $CO_2e$ ) or of including an undersown cover crop in the rotation between a winter and a spring crop to cover the soil in August–April (-444 kg  $CO_2e$ ) (Fig. 6). Considering only cultivated plots, the albedo-induced climate impact with  $GWP_{100}$  was up to -791 kg  $CO_2e$  for changing between crops, up to -578 kg  $CO_2e$  for cultivation of a winter-sown variety instead of a spring-sown variety of the same crop (here barley) and -171 kg  $CO_2e$  for late termination of ley grass. The potential benefit of an early-establishing, reflective cereal cultivar was estimated by comparing

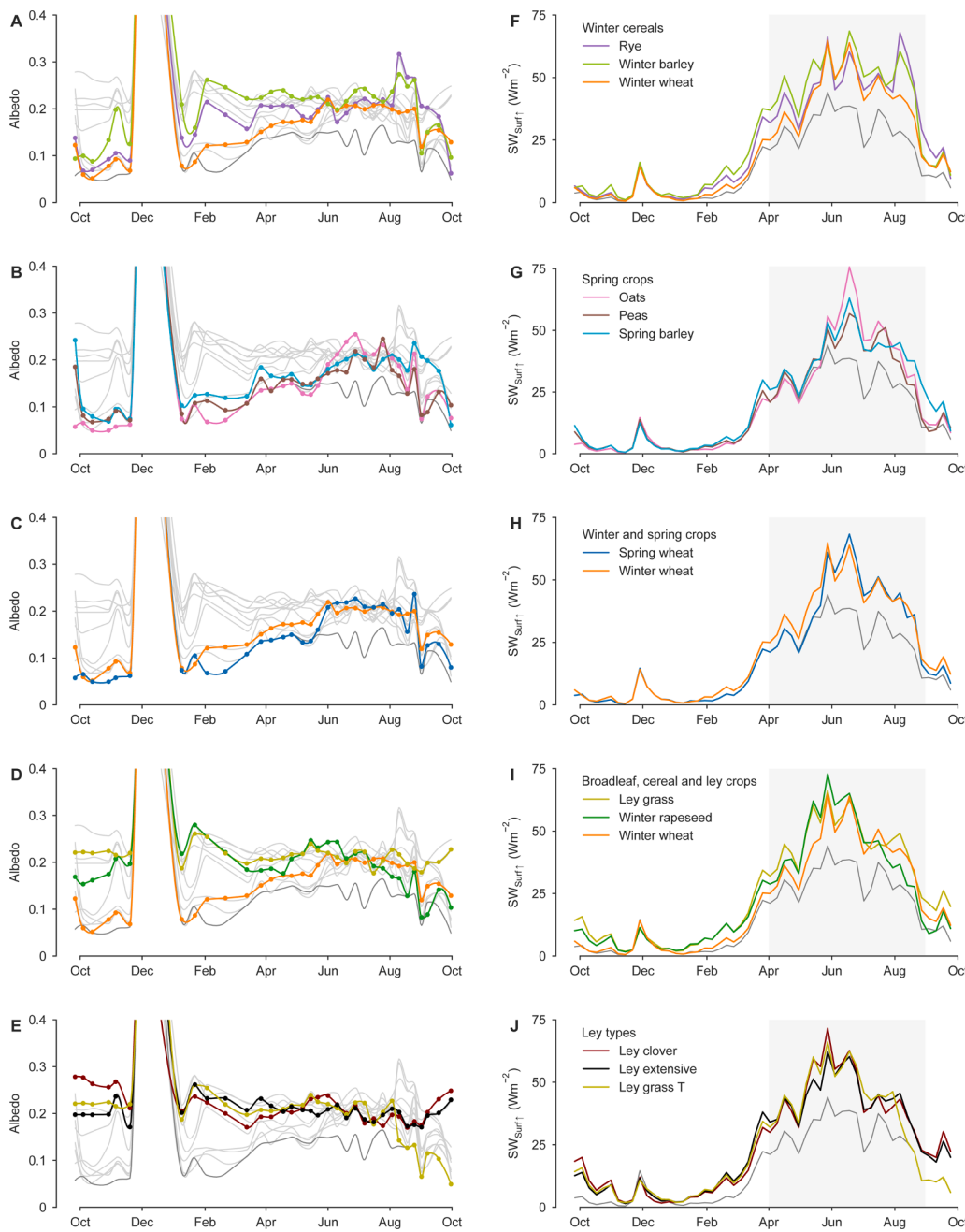


**Fig. 5.** Left (A-E): Daily albedo on selected plots including field-measured values (markers) and interpolated values (lines). Measured values with snow cover (0.55–0.95) are not shown. The dark grey line is bare soil and light grey lines represent all other plots included. Plots are grouped by expected similarity (e.g. A, B) and dissimilarity (e.g. C, D) of crops. Right (F-J): Up-welling shortwave irradiance at surface, shown as 7-day averages to smooth day-by-day variability resulting from changes in atmospheric properties. Inter-plot differences in net shortwave irradiance are approximately 25% lower because of enhanced downwelling irradiance over surfaces with high albedo. The shaded area indicates the period when a unit albedo change over the year would have 80% of its impact, due to high levels of incoming irradiance. Albedo differences in winter (e.g. due to snow cover) translated into very small forcings.

winter barley with winter rye, while accounting for differences in post-harvest management. In that case, the estimated cooling potential was -279 kg CO<sub>2</sub>e with GWP<sub>100</sub>.

Besides the land use and management options mentioned here, other anthropogenic and environmental factors could have contributed to the observed albedo differences between plots and calculated climate impacts, such as cultivated crop varieties, sowing and harvesting dates, fertilisation, residues left from the previous crop, soil moisture content, etc. Moreover, effect sizes may vary between fields and years due to soil composition and weather.

#### 3.4. Regional and inter-annual variations in albedo

A total of 1567 crop-specific MODIS pixels were found in Swedish agricultural production region PO4 across 10 years (Fig. S7a and Table S7b in SM). Comparison of field-measured albedo in Uppsala

2019–2020 with MODIS-derived albedo in PO4 2010–2020 showed that the observations for an individual site and year fell into the range of albedo values resulting from regional and inter-annual variation in growing conditions (Fig. 7). MODIS data for the same period were influenced by differing site characteristics and management, and data for 2010–2019 were also influenced by differences in yearly weather (e.g. precipitation, temperature, snow cover). For example, in 2012–2013 most crops had higher annual albedo than usual because the snow period extended until April. Differences between years shown here also included variation between sites, because pure pixels per crop are usually composed of different fields every year, at least for annual crops grown in a rotation. Fallow included both vegetated and unvegetated set-aside land, which explains why MODIS-derived albedo was between that of ley and bare soil. For ley, MODIS albedo included intensive, extensive, continued and terminated fields. It was much lower than field-measured albedo for ley in Uppsala.

**Table 3**

Annual albedo per plot, net shortwave irradiance at the surface and at the top of the atmosphere (TOA), and global climate impact of albedo change on one hectare during one year expressed as radiative forcing (RF) and as carbon dioxide equivalents (CO<sub>2</sub>e) using global warming potential (GWP) with time horizons of 100 and 20 years. RF and GWP shown here were calculated relative to bare soil. Values are mean (SD) of the Monte Carlo simulation results. T = terminated.

Albedo [-]	Net shortwave irradiance		Climate impact per hectare and year			
	$SW_{Surf,net}$ [Wm <sup>-2</sup> ]	$SW_{TOA,net}$ [Wm <sup>-2</sup> ]	RF [10 <sup>-11</sup> Wm <sup>-2</sup> ]	GWP <sub>100</sub> [kg CO <sub>2</sub> e]	GWP <sub>20</sub> [kg CO <sub>2</sub> e]	
Winter barley	0.222 (0.00092)	92.7 (0.087)	152.2 (0.062)	-11.0 (0.170)	-1202 (18.6)	-4418 (68.3)
Ley extensive (Ulleråker E)	0.216 (0.00091)	93.2 (0.087)	152.6 (0.062)	-10.2 (0.169)	-1113 (18.4)	-4091 (67.7)
Ley grass	0.215 (0.00091)	93.4 (0.086)	152.7 (0.061)	-10.0 (0.169)	-1087 (18.4)	-3997 (67.7)
Ley clover	0.209 (0.00092)	93.8 (0.087)	153.1 (0.062)	-9.3 (0.169)	-1019 (18.4)	-3746 (67.6)
Rye (Ultuna S)	0.209 (0.00092)	93.8 (0.087)	153.0 (0.062)	-9.5 (0.169)	-1035 (18.4)	-3804 (67.8)
Ley extensive	0.207 (0.00093)	94.1 (0.088)	153.2 (0.063)	-9.0 (0.170)	-980 (18.6)	-3602 (68.3)
Rye	0.206 (0.00092)	94.1 (0.087)	153.2 (0.062)	-9.1 (0.169)	-994 (18.4)	-3655 (67.6)
Ley grass T	0.201 (0.00092)	94.6 (0.087)	153.6 (0.062)	-8.2 (0.170)	-899 (18.5)	-3303 (68.0)
Winter rapeseed	0.200 (0.00091)	94.7 (0.086)	153.6 (0.061)	-8.3 (0.168)	-901 (18.3)	-3313 (67.3)
Winter wheat	0.182 (0.00092)	96.3 (0.086)	154.7 (0.061)	-6.1 (0.169)	-665 (18.4)	-2443 (67.6)
Spring barley	0.180 (0.00092)	96.5 (0.086)	154.9 (0.061)	-5.7 (0.168)	-624 (18.3)	-2295 (67.4)
Spring wheat	0.172 (0.00092)	97.2 (0.086)	155.3 (0.061)	-4.9 (0.168)	-535 (18.3)	-1965 (67.3)
Oats	0.171 (0.00092)	97.2 (0.086)	155.4 (0.061)	-4.8 (0.169)	-527 (18.4)	-1938 (67.7)
Peas	0.164 (0.00092)	98.0 (0.085)	155.9 (0.061)	-3.8 (0.170)	-411 (18.5)	-1512 (68.1)
Bare soil	0.134 (0.00092)	100.7 (0.084)	157.8 (0.060)	0	0	0

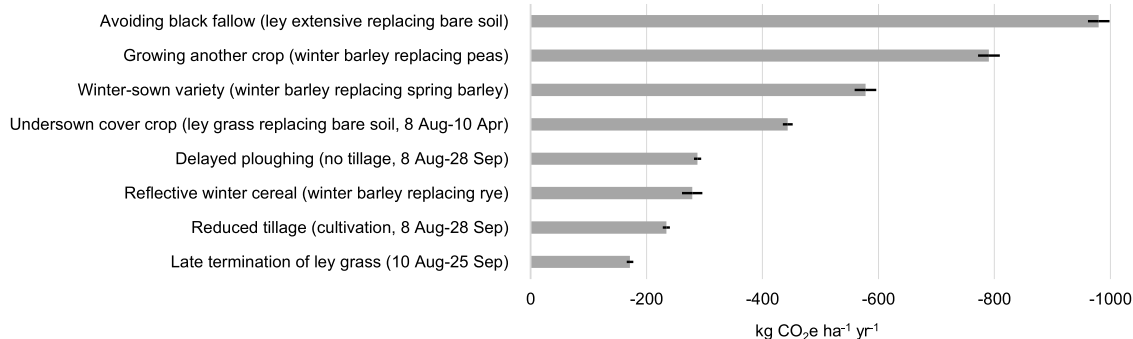


**Fig. 6.** Climate benefit of various measures to increase albedo on cropland per hectare and year, expressed as GWP<sub>100</sub>. Error bars show  $\pm$  one standard deviation of the Monte Carlo simulation results.

#### 4. Discussion

##### 4.1. Isolating effects of agricultural practices from other sources of variation

The albedo of cropland varies due to factors relating to soil type, meteorology and agricultural use and management. In fact, cropland and grassland show the highest albedo variations, both spatially and

temporally, of all vegetated IGBP classes, because of differences and rapid changes in vegetation (e.g. seasonal changes in leaf area index (LAI), response to temperature, water status and management), the fraction of exposed soil and soil moisture content (Cescatti et al., 2012; Gao et al., 2005). In the present study, different combinations of these factors led to great variability in the albedo of individual crops at regional level, despite similar pedo-climatic conditions in agricultural production region PO4. Crop-specific albedo obtained from the MODIS

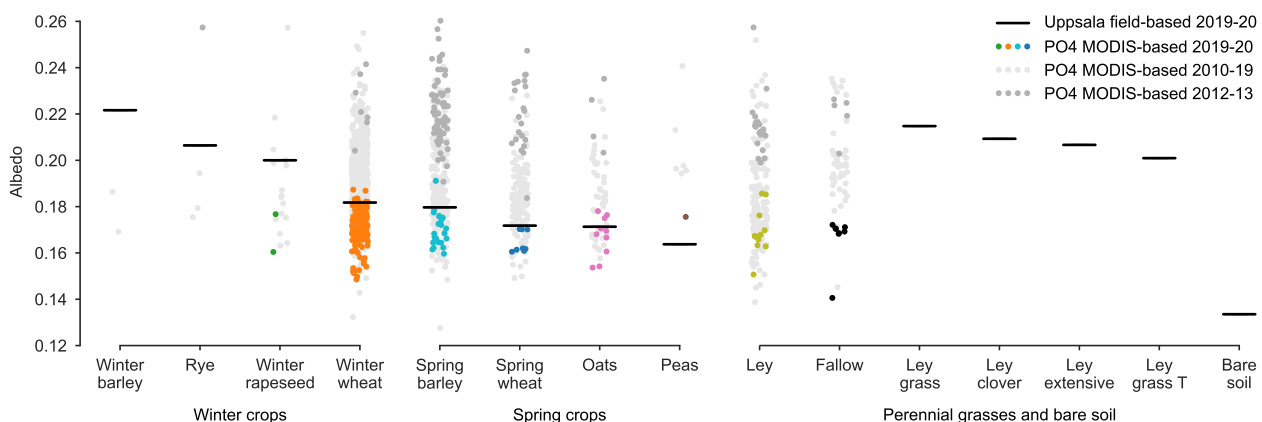


**Fig. 7.** Annual albedo for individual crops 2019-2020, based on field measurements in Uppsala (bars) and derived from pure MODIS pixels in Swedish agricultural production region PO4 during the same period (coloured dots) and in 2010-2019 (light grey dots). MODIS albedo in 2012-2013 is highlighted (dark grey dots) to illustrate inter-annual variation.

product proved useful for estimating the possible magnitude of variation across sites (i.e. pixels that may contain several fields with differing soil properties and management) and years. The method can be used to derive regionally representative albedo values per crop if many pure pixels are available (Sieber et al., 2022). Therefore, it is suitable for obtaining values for crops cultivated on large contiguous fields ( $>50$  ha, often 65–85 ha) in major agricultural regions and encompasses a mixture of prevalent management practices. Techniques have been developed for linearly unmixing the signal of heterogeneous MODIS pixels based on detailed land cover and management information (Bright & Astrup, 2019; Kuusinen et al., 2013). Such techniques could be used to derive management-specific albedo. However, challenges remain in obtaining accurate maps of yearly management, in modelling the observation footprint of MODIS pixels and in handling data gaps in winter at high latitudes. Moreover, MODIS albedo retrievals systematically underestimate the albedo of cropland and grassland, even over homogeneous areas of 100 ha, because they are likely to be surrounded by areas with lower albedo (Cescatti et al., 2012).

Paired field measurements enabled robust identification of management effects in this study. At field level and within years, observed differences between agricultural land uses and management practices were found to be determined mainly by two factors, phenology (i.e. fallow period, crop emergence and seasonal development, species composition) and post-harvest management (i.e. timing and intensity of tillage). Seasonal precipitation was shown to intensify or reduce differences between plots, depending on the degree of soil coverage with vegetation or residues and the impact on soil moisture. Pigglin and Schwerdtfeger (1973) concluded that differences between crops can be masked by differences in rainfall between individual years. On annual timescales, Miller et al. (2016) found a consistent ranking of crops across years and only small inter-annual variation. In years with abundant snowfall, all crops have higher albedo in winter and annual albedo shifts upward across crops (Miller et al., 2016; Sieber et al., 2022) (see Fig. 7). Multiple years (~10) of measurements would be needed to obtain representative values for the pedo-climatic conditions in Uppsala, and many sites would be needed to obtain representative values for different pedo-climatic conditions. Albedo values for the same crop can differ substantially across sites and latitudes (Breuer et al., 2003; Monteith and Unsworth, 2013).

The sampling strategy in this study allowed monitoring of 15 paired plots with a single set of instruments. This introduced some uncertainty compared with continuous measurements because short-term effects of precipitation might have been over- or under-represented, depending on when measurements were taken in relation to rain or snowfall events. Nevertheless, seasonal trends were in good agreement with findings by others of increasing albedo with growing plant cover (quantified as LAI or development from tillering to heading), a plateau at full plant cover, leaf drying decline (starting at the beginning of the maturity phase) due to increasing exposure of soil, and potentially an upturn at ripening (Miller et al., 2016; Pigglin & Schwerdtfeger, 1973; Zhang et al., 2013). Growing-season differences between crops were highest in autumn and spring (Fig. 3), when perennial ley and winter varieties had 0.05–0.2 higher albedo than spring crops. Full canopy albedo in summer was more similar across crops (0.21–0.25), as reported in previous studies (Eichelmann et al., 2016; Miller et al., 2016; Monteith & Unsworth, 2013). However, the timing and persistence of high albedo levels differed significantly. For example, winter rapeseed reached a full canopy in May and albedo declined from mid-June, whereas cereals reached their full canopy plateau later in summer and showed a weaker decline thereafter.

#### 4.2. Field-scale effects of agricultural practices on albedo and climate

The results in this study indicate that, in Northern Europe, crops with a long growing season have the highest annual albedo and thus the greatest mean annual cooling potential. This resulted mainly from

improved soil coverage in spring-summer for winter crops and also in autumn for perennial leys. Cover crops could be included in the rotation to increase albedo without affecting the main crops grown, with strong effects in regions with dark soil types and early harvesting dates (Carrer et al., 2018; Lugato et al., 2020). Potential climate benefits calculated for various measures to increase albedo on cropland in Uppsala (roughly up to  $-1000 \text{ kg CO}_2\text{e ha}^{-1} \text{ yr}^{-1}$ ) are of similar magnitude to the life cycle GHG impact of crop cultivation in Northern Europe, which is typically  $1200\text{--}2500 \text{ kg CO}_2\text{e ha}^{-1} \text{ yr}^{-1}$ , including fuel use for field operations ( $\sim 100\text{--}300 \text{ kg CO}_2\text{e}$ ), production of inputs (mainly mineral nitrogen fertiliser,  $\sim 300\text{--}800 \text{ kg CO}_2\text{e}$ ) and nitrous oxide emissions from soil ( $\sim 600\text{--}1500 \text{ kg CO}_2\text{e}$ ) (Börjesson & Tufvesson, 2011; Ceschia et al., 2010; Sieber et al., 2022). Over a shorter time horizon with GWP<sub>20</sub>, the climate impact of albedo change was 3.7 times as high as with GWP<sub>100</sub>. The GHG impact of crop cultivation is slightly lower with GWP<sub>20</sub>, due to dominance of long-lived GHGs ( $\text{N}_2\text{O}$  and  $\text{CO}_2$ ). Thus albedo increase through agricultural land use and management practices could offset a substantial proportion of RF deriving from field-level GHG emissions on short time-scales.

The choice of crop, due to differences in phenology, had important consequences for net shortwave irradiance and climate impacts on seasonal and annual time scales. During the spring-summer period, high albedo for winter barley was estimated to reduce  $SW_{\text{Surf},\text{net}}$  by at least  $1.3 \text{ W m}^{-2}$  (compared with winter rapeseed) and at most  $7.8 \text{ W m}^{-2}$  (compared with peas) (Table S5a in SM). Modelling studies that apply similar or smaller seasonal albedo increase and  $\Delta SW_{\text{Surf},\text{net}}$  on cropland at large scale found significant cooling of seasonal mean temperature (Georgescu et al., 2009; Georgescu et al., 2011), annual mean temperature (Lobell et al., 2006), daily maximum temperature (Doughty et al., 2011) and temperature peaks in summer (Davin et al., 2014). In June–July, when albedo increases could alleviate local heat stress, oats reduced  $SW_{\text{Surf},\text{net}}$  by  $0.8\text{--}5.8 \text{ W m}^{-2}$  compared with other cereals, ley, peas and rapeseed. However, albedo increases might not be desirable in early spring on cropland, when soil temperature and moisture restrict tillage and plant growth.

Outside the growing season of annual crops, residue retention from the preceding crop, timing of tillage (partly depending on the subsequent crop) and tillage intensity affected albedo. Remaining plant debris after shallow cultivation increased the albedo of unvegetated plots in October–March compared with ploughed plots, by 0.027 on the spring barley plot with residues of rapeseed and by 0.013 on the pea plot with residues of wheat. However, the impact on annual albedo and net shortwave irradiance was modest ( $\Delta SW_{\text{Surf},\text{net}}$  of  $-0.76$  and  $-0.36 \text{ W m}^{-2}$ , respectively), due to low incoming radiation. Effects of post-harvest management were strongest directly after the harvest of winter cereals. Under delayed ploughing, albedo was about 0.1 higher for two months because stubble and stalks were more reflective than the ploughed clay soil (Fig. 4, ‘No tillage’ vs. ‘Ploughed’). Under reduced tillage, albedo was about 0.05 higher for two months if both cultivation passes were performed directly after harvest, leaving a mixture of soil and plant debris (Fig. 4, ‘Cultivation 2x’ vs. ‘Ploughed’). When only stubble cultivation was performed directly after harvest, albedo was almost as high as on the untilled plot until the second cultivation pass (Fig. 4, ‘Cultivation’).

The effects of delayed ploughing and reduced tillage on albedo after harvest of cereals were similar in magnitude and duration to observations made elsewhere (Davin et al., 2014; O’Brien & Daigh, 2019). The albedo difference between stubble and ploughed plots (0.12, Table S6 in SM) was only slightly higher than in the study by Davin et al. (2014), despite the much lower albedo of ploughed clay soil. The albedo of stubble declined faster and more strongly on fields in the present study, most likely owing to rainfall and the underlying dark soil. Dark soil reduces the albedo of surfaces covered by crop residues or live vegetation, due to an uncovered fraction (Pigglin & Schwerdtfeger, 1973) and to partial transmission of radiation to the “background” (Pinty et al., 2006). Delayed ploughing of rye in this study was estimated to reduce

$SW_{Surf,net}$  by  $13.6 \text{ Wm}^{-2}$ . Implemented on one hectare during 52 days (8 Aug–28 Sep) in one cultivation year, the global climate benefit was -288 kg CO<sub>2</sub>e with GWP<sub>100</sub> (Table S6 in SM).

Overall, these results show that strategies to cool annual mean, seasonal and peak temperatures may prioritise different agricultural practices. The field plots in this study represented realistic management possibilities on present cropland, rather than functionally equal alternatives from an agronomic perspective. Nevertheless, the results improve understanding of the current variation in albedo on cropland, causes on seasonal time scales and direct effects on local and global energy budgets. This information can be used to predict outcomes of climate change mitigation and adaptation in agriculture, e.g. zonal and temporal shifts in crop species and varieties due to warmer growing seasons, soil coverage of temporal fallow, bioenergy, plant breeding, delayed or reduced tillage, etc.

#### 4.3. Limitations and future research

Besides effects on surface and TOA net shortwave irradiance, albedo change directly affects local moisture regimes by altering the amount of energy available for evapotranspiration. This can reduce cloud cover, with negative feedback on surface temperature due to increased incoming solar radiation and reduced precipitation (Doughty et al., 2011; Georgescu et al., 2011). Albedo increases achieved by agricultural management are also likely to be accompanied by changes in other biophysical variables, such as evaporation efficiency and surface roughness, which can amplify, dampen or reverse albedo-induced cooling.

Detailed knowledge about field-scale albedo, as obtained in this study, can support future efforts to improve the land surface representation in climate models (Lawrence et al., 2016; Pitman et al., 2009), to assess the climate impacts of land use and to design effective policies for climate change mitigation and adaptation (Anderson-Teixeira et al., 2012; Seneviratne et al., 2018; Smith et al., 2016). Given the high spatial and temporal variations in cropland albedo, more systematic data are needed for the robust quantification of management effects under a range of conditions. The present study showed that these variations cannot be explained by pedo-climatic conditions and crop types alone, but that accounting for species-specific phenology and management practices can greatly reduce uncertainty about the magnitude and seasonal patterns of cropland albedo.

#### 5. Conclusions

This study combined field- and satellite-based observations to analyse the magnitude and sources of variation in the albedo of cropland in a high-latitude temperate climate. At field level within years, albedo differed mainly depending on crop type, species-specific phenology and post-harvest management. Differences in observed albedo and in calculated net shortwave irradiance between plots had important effects on surface and TOA energy balances. Realistic changes in current agricultural practices to increase albedo could lead to benefits for global mean climate of -200 to -1000 kg CO<sub>2</sub>e ha<sup>-1</sup> yr<sup>-1</sup>, expressed as GWP<sub>100</sub>, and thus offset a substantial proportion of RF deriving from field-level GHG emissions on short time-scales. The regional climate could be influenced if similar albedo changes were implemented at larger scale on cropland. The experimental design in this study was too restricted to detect effects on local temperature, relative humidity and cloud formation, but field data can be used in modelling studies examining the effects of albedo increase on annual mean, seasonal or peak temperatures.

#### Declaration of Competing Interest

The authors declare that they have no known competing financial interests or personal relationships that could have appeared to influence

the work reported in this paper.

#### Acknowledgements

This work was supported by the Swedish strategic research programme STandUP for Energy. The authors would like to thank Åsa Myrbeck and Håkan Andersson (RISE), John Löfkvist (Dept. of Crop Production Ecology, SLU, and Lövsta research station) and Jarl Ryberg (Ultuna Egendom) for providing information on field sites and management. The results contain modified Copernicus Climate Change Service information 2021.

#### Supplementary materials

Supplementary material associated with this article can be found, in the online version, at doi:[10.1016/j.agrformet.2022.108978](https://doi.org/10.1016/j.agrformet.2022.108978).

#### References

- Akima, H., 1970. A New Method of Interpolation and Smooth Curve Fitting Based on Local Procedures. *J. ACM* 17 (4), 589–602. <https://doi.org/10.1145/321607.321609>.
- Anderson-Teixeira, K.J., Snyder, P.K., Twine, T.E., Cuadra, S.V., Costa, M.H., DeLucia, E.H., 2012. Climate-regulation services of natural and agricultural ecoregions of the Americas. *Nature Climate Change* 2 (3), 177–181. <https://doi.org/10.1038/nclimate1346>.
- Andrén, O., Kätterer, T., Karlsson, T., Eriksson, J., 2008. Soil C balances in Swedish agricultural soils 1990–2004, with preliminary projections. *Nutr. Cycling Agroecosyst.* 81 (2), 129–144. <https://doi.org/10.1007/s10705-008-9177-z>.
- Bala, G., Caldeira, K., Wickett, M., Phillips, T.J., Lobell, D.B., Delire, C., Mirin, A., 2007. Combined climate and carbon-cycle effects of large-scale deforestation. *Proc. Nat. Acad. Sci. United States Am.* 104 (16), 6550–6555. <https://doi.org/10.1073/pnas.0608998104>.
- Betts, R.A., Falloon, P.D., Goldeijk, K.K., Ramankutty, N., 2007. Biogeophysical effects of land use on climate: Model simulations of radiative forcing and large-scale temperature change. *Agric. For. Meteorol.* 142 (2–4), 216–233. <https://doi.org/10.1016/j.agrformet.2006.08.021>.
- Bonan, G., 2015. *Ecological Climatology: Concepts and Applications*, 3 ed. Cambridge University Press, Cambridge.
- Breuer, L., Eckhardt, K., Frede, H.-G., 2003. Plant parameter values for models in temperate climates. *Ecol. Modell.* 169 (2), 237–293. [https://doi.org/10.1016/S0304-3800\(03\)00274-6](https://doi.org/10.1016/S0304-3800(03)00274-6).
- Bright, R.M., Astrup, R., 2019. Combining MODIS and National Land Resource Products to Model Land Cover-Dependent Surface Albedo for Norway. *Remote Sensing* 11 (7). <https://doi.org/10.3390/rs11070871>.
- Bright, R.M., Cherubini, F., Stromman, A.H., 2012. Climate impacts of bioenergy: Inclusion of carbon cycle and albedo dynamics in life cycle impact assessment. *Environ. Impact Assess. Rev.* 37, 2–11. <https://doi.org/10.1016/j.eiar.2012.01.002>.
- Bright, R.M., Lund, M.T., 2021. CO<sub>2</sub>-equivalence metrics for surface albedo change based on the radiative forcing concept: a critical review. *Atmos. Chem. Phys.* 21 (12), 9887–9907. <https://doi.org/10.5194/acp-21-9887-2021>.
- Bright, R.M., Zhao, K.G., Jackson, R.B., Cherubini, F., 2015. Quantifying surface albedo and other direct biogeophysical climatic forcings of forestry activities. *Global Change Biol.* 21 (9), 3246–3266. <https://doi.org/10.1111/gcb.12951>.
- Börjesson, P., Tufvesson, L.M., 2011. Agricultural crop-based biofuels – resource efficiency and environmental performance including direct land use changes. *J. Cleaner Prod.* 19 (2), 108–120. <https://doi.org/10.1016/j.jclepro.2010.01.001>.
- Cai, H., Wang, J., Feng, Y., Wang, M., Qin, Z., Dunn, J.B., 2016. Consideration of land use change-induced surface albedo effects in life-cycle analysis of biofuels. *Energy Environ. Sci.* 9 (9), 2855–2867. <https://doi.org/10.1039/c6ee01728b>.
- Caiazzo, F., Malina, R., Staples, M.D., Wolfe, P.J., Yim, S.H.L., Barrett, S.R.H., 2014. Quantifying the climate impacts of albedo changes due to biofuel production: a comparison with biogeochemical effects. *Environ. Res. Lett.* 9 (2) <https://doi.org/10.1088/1748-9326/9/2/024015>.
- Carrer, D., Pique, G., Ferlicoq, M., Ceamanos, X., Ceschia, E., 2018. What is the potential of cropland albedo management in the fight against global warming? A case study based on the use of cover crops. *Environ. Res. Lett.* 13 (4) <https://doi.org/10.1088/1748-9326/aa6505>.
- Cescatti, A., Marcolla, B., Santhana Vannan, S.K., Pan, J.Y., Román, M.O., Yang, X., Ciais, P., Cook, R.B., Law, B.E., Matteucci, G., Migliavacca, M., Moors, E., Richardson, A.D., Seufert, G., Schaaf, C.B., 2012. Intercomparison of MODIS albedo retrievals and in situ measurements across the global FLUXNET network. *Remote Sens. Environ.* 121, 323–334. <https://doi.org/10.1016/j.rse.2012.02.019>.
- Ceschia, E., Bézat, P., Dejoux, J.F., Aubinet, M., Bernhofer, C., Bodson, B., Buchmann, N., Carrara, A., Cellier, P., Di Tommasi, P., Elbers, J.A., Eugster, W., Grünwald, T., Jacobs, C.M.J., Jans, W.W.P., Jones, M., Kutsch, W., Lanigan, G., Magliulo, E., Marloie, O., Moors, E.J., Moureaux, C., Olioso, A., Osborne, B., Sanz, M.J., Saunders, M., Smith, P., Soegaard, H., Wattenbach, M., 2010. Management effects on net ecosystem carbon and GHG budgets at European crop sites. *Agricult., Ecosyst. Environ.* 139 (3), 363–383. <https://doi.org/10.1016/j.agee.2010.09.020>.

- Davin, E.L., de Noblet-Ducoudré, N., 2010. Climatic Impact of Global-Scale Deforestation: Radiative versus Nonradiative Processes. *Journal of Climate* 23 (1), 97–112. <https://doi.org/10.1175/2009JCLI3102.1>.
- Davin, E.L., Seneviratne, S.I., Ciais, P., Olioso, A., Wang, T., 2014. Preferential cooling of hot extremes from cropland albedo management. In: *Proceedings of the National Academy of Sciences of the United States of America*, 111, pp. 9757–9761. <https://doi.org/10.1073/pnas.1317323111>.
- Doughty, C.E., Field, C.B., McMillan, A.M.S., 2011. Can crop albedo be increased through the modification of leaf trichomes, and could this cool regional climate? *Clim. Change* 104 (2), 379–387. <https://doi.org/10.1007/s10584-010-9936-0>.
- Duveiller, G., Baret, F., Defourny, P., 2011. Crop specific green area index retrieval from MODIS data at regional scale by controlling pixel-target adequacy. *Remote Sens. Environ.* 115 (10), 2686–2701. <https://doi.org/10.1016/j.rse.2011.05.026>.
- Erb, K.-H., Luyssaert, S., Meyfroidt, P., Pongratz, J., Don, A., Kloster, S., Kuemmerle, T., Fetz, T., Fuchs, R., Herold, M., Haberl, H., Jones, C.D., Marín-Spiotta, E., McCallum, I., Robertson, E., Seufert, V., Fritz, S., Valade, A., Wiltshire, A., Dolman, A.J., 2017. Land management: data availability and process understanding for global change studies. *Global Change Biol.* 23 (2), 512–533. <https://doi.org/10.1111/gcb.13443>.
- Gao, F., He, T., Wang, Z., Ghimire, B., Shuai, Y., Masek, J., Schaaf, C., Williams, C., 2014. Multiscale climatological albedo look-up maps derived from moderate resolution imaging spectroradiometer BRDF/albedo products. *J. Appl. Remote Sens.* 8 (1), 083532. <https://doi.org/10.1117/1.JRS.8.083532>.
- Gao, F., Schaaf, C.B., Strahler, A.H., Roesch, A., Lucht, W., Dickinson, R., 2005. MODIS bidirectional reflectance distribution function and albedo Climate Modeling Grid products and the variability of albedo for major global vegetation types. *J. Geophys. Res.* 110 (D1) <https://doi.org/10.1029/2004JD005190>.
- Genesio, L., Bassi, R., Miglietta, F., 2021. Plants with less chlorophyll: A global change perspective. *Global Change Biol.* 27 (5), 959–967. <https://doi.org/10.1111/gcb.15470>.
- Georgescu, M., Lobell, D.B., Field, C.B., 2009. Potential impact of U.S. biofuels on regional climate. *Geophys. Res. Lett.* 36 (21) <https://doi.org/10.1029/2009GL040477>.
- Georgescu, M., Lobell, D.B., Field, C.B., 2011. Direct climate effects of perennial bioenergy crops in the United States. In: *Proceedings of the National Academy of Sciences of the United States of America*, 108, pp. 4307–4312. <https://doi.org/10.1073/pnas.1008779108>.
- Hersbach, H., Bell, B., Berrisford, P., Horányi, A., Muñoz Sabater, J., Nicolas, J., Radu, R., Schepers, D., Simmons, A., Soci, C., & Dee, D. (2018). ERA5 hourly data on single levels from 1979 to present [Online dataset]. Copernicus Climate Change Service (C3S) Climate Data Store (CDS). doi:[10.24381/cds.adbb2d47](https://doi.org/10.24381/cds.adbb2d47).
- Hollinger, D.Y., Ollinger, S.V., Richardson, A.D., Meyers, T.P., Dail, D.B., Martin, M.E., Scott, N.A., Arkebauer, T.J., Baldocchi, D.D., Clark, K.L., Curtis, P.S., Davis, K.J., Desai, A.R., Dragoni, D., Goulden, M.L., Gu, L., Katul, G.G., Pallardy, S.G., Paw, K.T., Schmid, H.P., Stoy, P.C., Suyker, A.E., Verma, S.B., 2010. Albedo estimates for land surface models and support for a new paradigm based on foliage nitrogen concentration. *Global Change Biol.* 16 (2), 696–710. <https://doi.org/10.1111/j.1365-2486.2009.02028.x>.
- Kaye, J.P., Quemada, M., 2017. Using cover crops to mitigate and adapt to climate change. A review. *Agron. Sustainable Dev.* 37 (1), 4. <https://doi.org/10.1007/s13593-016-0410-x>.
- Kuusinen, N., Tomppo, E., Berninger, F., 2013. Linear unmixing of MODIS albedo composites to infer subpixel land cover type albedos. *Int. J. Appl. Earth Obs. Geoinf.* 23, 324–333. <https://doi.org/10.1016/j.jag.2012.10.005>.
- Lawrence, D.M., Hurtt, G.C., Arneth, A., Brovkin, V., Calvin, K.V., Jones, A.D., Jones, C.D., Lawrence, P.J., de Noblet-Ducoudré, N., Pongratz, J., Seneviratne, S.I., Sheviakova, E., 2016. The Land Use Model Intercomparison Project (LUMIP) contribution to CMIP6: rationale and experimental design. *Geosci. Model Dev.* 9 (9), 2973–2998. <https://doi.org/10.5194/gmd-9-2973-2016>.
- Lenton, T.M., Vaughan, N.E., 2009. The radiative forcing potential of different climate geoengineering options. *Atmos. Chem. Phys.* 9 (15), 5539–5561. <https://doi.org/10.5194/acp-9-5539-2009>.
- Liu, J., Worth, D.E., Desjardins, R.L., Haak, D., McConkey, B., Cerkowniak, D., 2021. Influence of two management practices in the Canadian Prairies on radiative forcing. *Sci. Total Environ.* 765, 142701 <https://doi.org/10.1016/j.scitotenv.2020.142701>.
- Lobell, D.B., Bala, G., Duffy, P.B., 2006. Biogeophysical impacts of cropland management changes on climate. *Geophys. Res. Lett.* 33 (6) <https://doi.org/10.1029/2005GL025492>.
- Lugato, E., Cescatti, A., Jones, A., Ceccherini, G., Duveiller, G., 2020. Maximising climate mitigation potential by carbon and radiative agricultural land management with cover crops. *Environ. Res. Lett.* 15 (9), 094075 <https://doi.org/10.1088/1748-9326/aba137>.
- Mahmood, R., Pielke, R.A., Hubbard, K.G., Niyogi, D., Dirmeyer, P.A., McAlpine, C., Carleton, A.M., Hale, R., Gameda, S., Beltran-Przekurat, A., Baker, B., McNider, R., Legates, D.R., Shepherd, M., Du, J.Y., Blanken, P.D., Frauenfeld, O.W., Nair, U.S., Fall, S., 2014. Land cover changes and their biogeophysical effects on climate. *Int. J. Climatol.* 34 (4), 929–953. <https://doi.org/10.1002/joc.3736>.
- Miller, J.N., VanLoocke, A., Gomez-Casanovas, N., Bernacchi, C.J., 2016. Candidate perennial bioenergy grasses have a higher albedo than annual row crops. *GCB Bioenergy* 8 (4), 818–825. <https://doi.org/10.1111/gcb.12291>.
- Monteith, J.L., Unsworth, M.H., 2013. Chapter 6 - microclimatology of radiation: (i) radiative properties of natural materials. In: Monteith, J.L., Unsworth, M.H. (Eds.), *Principles of Environmental Physics*, 4th Ed. Academic Press, Boston, pp. 81–93.
- O'Brien, P.L., Daigh, A.L.M., 2019. Tillage practices alter the surface energy balance – A review. *Soil Tillage Res.* 195, 104354 <https://doi.org/10.1016/j.still.2019.104354>.
- Pielke, R.A., Avissar, R., Raupach, M., Dolman, A.J., Zeng, X.B., Denning, A.S., 1998. Interactions between the atmosphere and terrestrial ecosystems: influence on weather and climate. *Global Change Biol.* 4 (5), 461–475. <https://doi.org/10.1046/j.1365-2486.1998.t01-1-00176.x>.
- Piggott, I., Schwerdtfeger, P., 1973. Variations in the albedo of wheat and barley crops. *Archiv für Meteorologie, Geophysik und Bioklimatologie, Serie B* 21 (4), 365–391. <https://doi.org/10.1007/BF02253314>.
- Pinty, B., Lavergne, T., Dickinson, R.E., Widlowski, J.-L., Gobron, N., Verstraete, M.M., 2006. Simplifying the interaction of land surfaces with radiation for relating remote sensing products to climate models. *J. Geophys. Res.* 111 (D2) <https://doi.org/10.1029/2005JD005952>.
- Pitman, A.J., de Noblet-Ducoudré, N., Cruz, F.T., Davin, E.L., Bonan, G.B., Brovkin, V., Claussen, M., Delire, C., Ganzeveld, L., Gayler, V., van den Hurk, B.J.J.M., Lawrence, P.J., van der Molen, M.K., Müller, C., Reick, C.H., Seneviratne, S.I., Strengers, B.J., Voldoire, A., 2009. Uncertainties in climate responses to past land cover change: First results from the LUCID intercomparison study. *Geophys. Res. Lett.* 36 (14) <https://doi.org/10.1029/2009GL039076>.
- Qu, Y., Liang, S., Liu, Q., He, T., Liu, S., Li, X., 2015. Mapping surface broadband albedo from satellite observations: a review of literatures on algorithms and products. *Remote Sensing* 7 (1), 990–1020. <https://doi.org/10.3390/rs7010090>.
- Schaaf, C.B., & Wang, Z. (2015). *MCD43A1 MODIS/Terra+Aqua BRDF/Albedo Model Parameters Daily L3 Global - 500m V006* [Online dataset]. NASA EOSDIS Land Processes DAAC. doi:[10.5067/MODIS/MCD43A1.006](https://doi.org/10.5067/MODIS/MCD43A1.006).
- Seneviratne, S.I., Phipps, S.J., Pitman, A.J., Hirsch, A.L., Davin, E.L., Donat, M.G., Hirsch, M., Lenton, A., Wilhelm, M., Kravitz, B., 2018. Land radiative management as contributor to regional-scale climate adaptation and mitigation. *Nat. Geosci.* 11 (2), 88–96. <https://doi.org/10.1038/s41561-017-0057-5>.
- Sieber, P., Ericsson, N., Hammar, T., Hansson, P.-A., 2020. Including albedo in time-dependent LCA of bioenergy. *GCB Bioenergy* 12 (6), 410–425. <https://doi.org/10.1111/gcb.12682>.
- Sieber, P., Ericsson, N., Hammar, T., Hansson, P.-A., 2022. Albedo impacts of agricultural land use: Crop-specific albedo from MODIS data and inclusion in LCA of crop production. *Sci. Total Environ.* 155455 <https://doi.org/10.1016/j.scitotenv.2022.155455>.
- Sieber, P., Ericsson, N., Hansson, P.-A., 2019. Climate impact of surface albedo change in Life Cycle Assessment: Implications of site and time dependence. *Environ. Impact Assess. Rev.* 77, 191–200. <https://doi.org/10.1016/j.eiar.2019.04.003>.
- Singarayer, J.S., Davies-Barnard, T., 2012. Regional climate change mitigation with crops: context and assessment. *Philos. Trans. R. Soc., A* 370 (1974), 4301–4316. <https://doi.org/10.1098/rsta.2012.0010>.
- Smith, P., 2016. Soil carbon sequestration and biochar as negative emission technologies. *Global Change Biol.* 22 (3), 1315–1324. <https://doi.org/10.1111/gcb.13178>.
- Smith, P., Davis, S.J., Creutzig, F., Fuss, S., Minx, J., Gabrielle, B., Kato, E., Jackson, R.B., Cowie, A., Kriegler, E., van Vuuren, D.P., Rogelj, J., Ciais, P., Milne, J., Canadell, J.G., McCollum, D., Peters, G., Andrew, R., Krey, V., Shrestha, G., Friedlingstein, P., Gasser, T., Grübler, A., Heidug, W.K., Jonas, M., Jones, C.D., Kraxner, F., Littleton, E., Lowe, J., Moreira, J.R., Nakicenovic, N., Obersteiner, M., Patwardhan, A., Rognes, M., Rubin, E., Sharifi, A., Torvanger, A., Yamagata, Y., Edmonds, J., Yongsung, C., 2016. Biophysical and economic limits to negative CO<sub>2</sub> emissions. *Nature Climate Change* 6 (1), 42–50. <https://doi.org/10.1038/nclimate2870>.
- Stephens, G.L., O'Brien, D., Webster, P.J., Pilewski, P., Kato, S., Li, J.L., 2015. The albedo of Earth. *Rev. Geophys.* 53 (1), 141–163. <https://doi.org/10.1002/2014rg000449>.
- von Harden, A.C., Marín-Spiotta, E., Jackson, R.D., Kucharlik, C.J., 2019. Soil microclimates influence annual carbon loss via heterotrophic soil respiration in maize and switchgrass bioenergy cropping systems. *Agric. For. Meteorol.* 279, 107731 <https://doi.org/10.1016/j.agrformet.2019.107731>.
- Wang, Z., Schaaf, C.B., Sun, Q., Shuai, Y., & Román, M.O., 2018. Capturing rapid land surface dynamics with Collection V006 MODIS BRDF/NBAR/Albedo (MCD43) products. *Remote Sensing of Environment*, 207, 50–64. doi:[10.1016/j.rse.2018.02.001](https://doi.org/10.1016/j.rse.2018.02.001).
- Wilhelm, M., Davin, E.L., Seneviratne, S.I., 2015. Climate engineering of vegetated land for hot extremes mitigation: an Earth system model sensitivity study. *J. Geophys. Res.* 120 (7), 2612–2623. <https://doi.org/10.1002/2014JD022293>.
- Williamson, S.N., Barrio, I.C., Hik, D.S., Gamon, J.A., 2016. Phenology and species determine growing-season albedo increase at the altitudinal limit of shrub growth in the sub-Arctic. *Global Change Biol.* 22 (11), 3621–3631. <https://doi.org/10.1111/gcb.13297>.
- Winton, M., 2005. Simple optical models for diagnosing surface-atmosphere shortwave interactions. *J. Climate* 18 (18), 3796–3805. <https://doi.org/10.1175/jcli3502.1>.
- Zhang, Y.-f., Wang, X.-p., Pan, Y.-x., Hu, R., 2013. Diurnal and seasonal variations of surface albedo in a spring wheat field of arid lands of Northwestern China. *Int. J. Biometeorol.* 57 (1), 67–73. <https://doi.org/10.1007/s00484-012-0534-x>.